INSTITUTE FOR FUSION STUDIES

Enhanced Pinch Effect due to Electrostatic Potential

K.C. Shaing
Oak Ridge National Laboratory
Oak Ridge, Tennessee   37831
and
R.D. Hazeltine
Institute for Fusion Studies and Department of Physics
The University of Texas at Austin
Austin, Texas   78712

January 1990

THE UNIVERSITY OF TEXAS

AUSTIN

Enhanced Pinch Effect due to Electrostatic Potential [a]

K.C. Shaing

Oak Ridge National Laboratory

Oak Ridge, Tennessee 37831

and

R.D. Hazeltine

Institute for Fusion Studies and Department of Physics

The University of Texas at Austin

Austin, Texas 78712

Abstract

An inward particle pinch appears necessary to explain experimental results in tokamaks. Neither the neoclassical pinch effect, which is too small, nor the off-diagonal quasilinear term, which is usually outward in the trapped particle regime, can account for the observations. A mechanism for an enhanced inward pinch is proposed, based on results for an asymmetric magnetic field bump [R.D. Hazeltine and M.N. Rosenbluth, Phys. Fluids **15**, 2211 (1972)]. Because turbulent fluctuations also break toroidal symmetry, an enhanced inward pinch driven by the fluctuations and the Ohmic inductive field, E is expected. To demonstrate this effect, an inward particle flux is calculated for a model tokamak configuration that has an electrostatic potential bump Φ_0 at toroidal angle $\zeta = 2\pi$. For the parameter regime $r/R < e\Phi_0/T_e < 1$, the flux is found to be $\Gamma = -4.47K(q)(r/R)L(\Phi_0)(v_{te}/R\nu e)^{1/2}cNE/B$, where $r(R)$ is minor (major) radius, B is the magnetic field strength, v_{te} is the electron thermal speed, ν_e is the electron-ion

collision frequency, q is the safety factor, and $K(q)$ and $L(\Phi_0)$ are functions of q and Φ_0 respectively. The results are also applicable to an asymmetric potential bump created externally to enhance the inward pinch flux of high energy, collisionless particles.

I. Introduction

There appears to be strong evidence for the existence of an anamolous inward pinch in tokamak particle confinement. It is known that an inward particle pinch is required to explain the existence of peaked density profiles in the core of edge-fueled Ohmic plasmas.[1,2] Particle diffusivity inferred from sawtooth density pulse propagation and from oscillating gas puff experiments is larger than that inferred from the steady state particle balance, which implies the existence of an inward pinch.[3,4] The magnitude of the required inward pinch velocity is generally larger than that of the neoclassical pinch.[5] Even though the combination of an anomalous diffusivity and the neoclassical pinch seems adequate to explain the central density profile evolution after pellet injection in JET (Joint European Tokamak), an anomalous pinch may still be needed in the edge region.[6]

Theoretical understanding of the origin of the anomalous pinch is mainly based on quasi-linear theory. In the plateau regime where $\nu_{*e} = \nu_e R q / (v_{te} \epsilon^{3/2}) > 1$, with ν_e the electron-electron collision frequency, v_{te} the thermal speed, R the major radius, q, the safety factor, and ϵ, the inverse aspect ratio, there is an inward pinch term associated with the electron temperature gradient for the ion mixing mode.[7] However, when $\nu_{*e} < 1$, the flux is usually outward for $\nu_{\text{eff}} = (\nu_e/\epsilon) > \omega_{*e}$, the electron diamagnetic drift frequency.[8] A recent calculation indicates that an inward particle flux can exist if $\nu_{\text{eff}} < 0.78 \omega_{*e}$.[9] Because such an inward flux only exists for high temperature plasmas, one needs to consider an alternative mechanism.

We propose here an enhanced inward pinch mechanism in the trapped particle regime due to the asymmetric electrostatic potential. Because electrostatic potential fluctuations are ubiquitous in tokamaks, and they break the toroidal symmetry, it is therefore interesting to calculate the inward pinch in the presence of the symmetry breaking electrostatic potential fluctuations. From a previous study on the enhanced trapped particle pinch velocity due

to the asymmetric magnetic bump,[10] one expects the pinch velocity to be enhanced due to the electrostatic fluctuations. To simplify the analysis, we calculate the pinch velocity in a tokamak with an electrostatic potential bump located at the toroidal angle $\zeta = 0$. The model is therefore similar to that for the asymmetric magnetic bump. Even though the frequency (v_{te}/R) with which particle encounters the potential bump in the model is different from the frequency $(v_{te}|m - nq|/Rq)$ in a realistic situation where the perturbation has a poloidal mode number m and a toroidal mode number n, the model does describe the crucial features of trapping and boundary layer formation required for an enhanced inward pinch flux. Because the pinch flux calculated here is driven by the Ohmic inductive electric field, it does not depend critically on the specific type of instability involved but the mode frequency has to be lower than ν_{eff}. The model can also be employed to describe the pinch effect of electrostatic potential created by a poloidal limiter or other means located at $\zeta = 0$.

This paper is organized as follows. In Sec. II, we describe the model and the drift kinetic equation to be used. The solution of the kinetic equation and the inward particle flux are given in Sec. III. The concluding remarks are given in Sec. IV.

II. Model and Drift Kinetic Equation

We assume that there there is a zero-width electrostatic potential bump located at $\zeta = 0$ with height Φ_0 in a tokamak magnetic geometry. The potential is assumed to be static in time. It could therefore be used either to simulate the low frequency fluctuations with mode frequency $\omega \ll \nu_{\text{eff}}$, or to describe a poloidal limiter. To simplify the analysis, we employ the ordering $1 > e\Phi_0/T_e > \epsilon$ with e the electric charge and T_e the electron temperature. To the lowest order in $\epsilon T_e/e\Phi_0 < 1$, trapped particles are trapped in the potential bump. Whether a particle will be trapped in the potential bump depends on its pitch angle parameter which is defined as $\lambda = \mu/w$, where μ is the magnetic moment, $w = v^2/2$, and v the particle speed. If $\lambda > \lambda_c \equiv [(w - w_0)/w]$, the particle is trapped, otherwise it is not. Here we use

$w_0 = e\Phi_0/M$ with M the mass of the particle as the normalized potential height.

To calculate the inward pinch flux, we must solve the linearized drift kinetic equation for the particle distribution function f

$$\sigma u \hat{n} \cdot \boldsymbol{\nabla} f - C(f) = -V_{dr} \frac{df_M}{dr} - \frac{eE}{T_e} \sigma u \, f_M \, , \tag{1}$$

where $\hat{n} = \mathbf{B}/B$, $\mathbf{B}$ is the magnetic field, $B = |\mathbf{B}|$, $\sigma = \pm 1$ is the sign of the parallel (to $\mathbf{B}$) velocity $v_\parallel \hat{n}$, $u = |v_\parallel|$, E is the Ohmic inductive electric field, and f_M is the Maxwellian distribution.[11] The radial drift velocity V_{dr} can be expressed as

$$V_{dr} = -\frac{Mc}{eB} u \, \mathbf{B} \times \boldsymbol{\nabla} r \cdot \boldsymbol{\nabla} \left(\frac{u}{B} \right), \, 0 < \zeta < 2\pi \, . \tag{2}$$

For simplicity, we employ the Lorentz operator

$$C(f) = \nu \frac{u}{w} \frac{\partial}{\partial \lambda} u \lambda \frac{\partial f}{\partial \lambda} \, , \tag{3}$$

where ν is the combined electron-electron and electron-ion collision frequency. For this simple model, we can impose exact boundary conditions. For circulating particles, f must be continuous across the potential bump

$$f_\sigma(\zeta = 0) = f_\sigma(\zeta = 2\pi) \, , \, \lambda < \lambda_c \, . \tag{4}$$

The σ dependence in f is denoted by the subscript. For trapped particles, f must satisfy the reflection boundary condition:

$$f_+(\zeta = 0) = f_-(\zeta = 0); \quad f_+(\zeta = 2\pi) = f_-(\zeta = 2\pi), \quad \text{for} \quad \lambda > \lambda_c \, . \tag{5}$$

III. Boundary Layer

In this section we solve Eq. (1) approximately, for small collision frequency. For simplicity we consider only the driving term proportional to E.

Because of the consistency (Dreicer) condition $E = \mathcal{O}(\nu)$, the lowest order version of (1) requires $\mathbf{n} \cdot \nabla f^0 = 0$. Thus, in view of Eqs. (4) and (5), f^0 must be independent of angle in the untrapped region:

$$f^0 = G(r, \mathbf{v}) \qquad , \qquad \lambda < \lambda_c \ .$$

In the trapped region, on the other hand, a solution of the form

$$f^0 = H(r, q\zeta - \theta, \mathbf{v}) \qquad , \qquad \lambda > \lambda_c \ ,$$

is permissible. Notice that the function H extends across the entire trapped region. For this reason, and because of its θ-dependence, H importantly affects the radial particle flux. Indeed we will find that the asymmetrical pinch effect results entirely from H.

Proceeding to next order we find

$$\sigma u \mathbf{n} \cdot \nabla f^1 - \nu \left(\frac{u}{w} \right) \left(\frac{\partial}{\partial \lambda} \right) \left(\frac{u\lambda}{\partial \lambda} \frac{\partial f^0}{\partial \lambda} \right) = - \left(\frac{eE}{T} \right) \sigma u f_M \ .$$

After averaging this equation over the lowest order trajectory, we obtain the solubility conditions,

$$-\sigma \left(\frac{\partial}{\partial \lambda} \right) \left(\frac{\langle uB \rangle \lambda \partial G}{\partial \lambda} \right) = - \left(\frac{e \langle EB \rangle}{T} \right) \left(\frac{w}{\nu} \right) f_M \qquad , \qquad \lambda < \lambda_c$$

in the untrapped region, and

$$\frac{\partial H}{\partial \lambda} = 0 \qquad , \qquad \lambda > \lambda_c$$

in the trapped region, since the Ohmic field has no bounce average. Here the angular brackets denote a flux-surface average whose explicit form is given in Section IV. In summary, the lowest order solution is given by

$$f = \left(\frac{eE}{T} \right) \left(\frac{w}{\nu} \right) f_M \int_\lambda^{\lambda_c} \frac{d\lambda}{\langle u \rangle} \qquad , \qquad \lambda < \lambda_c \tag{6}$$

$$f = H(r, q\zeta - \theta, w) \qquad , \qquad \lambda > \lambda_c \ . \tag{7}$$

6

Here we have simplfied the θ-averages in a conventional way, keeping the θ-dependence in u, which contributes in order $(r/R)^{1/2}$, but neglecting (r/R)-corrections in B and E.

It is clear that (6) and (7) specify a function that is discontinuous across the trapped-untrapped boundary. Thus there arises a velocity-space boundary layer, in which sharp λ-variation defeats the nominal banana-regime ordering. The function H, while not localized to the layer, is nonetheless determined by boundary layer physics. Because of the importance of H, we proceed next to analyze the boundary layer.

In the interior of the boundary layer, $\lambda \approx \lambda_c$, Eq. (1) is approximated by

$$\sigma \left[\frac{\partial f}{\partial \zeta} + \left(\frac{1}{q} \right) \frac{\partial f}{\partial \theta} \right] - \left(\frac{\nu R}{wB} \right) \frac{\partial}{\partial \lambda} \left[\frac{u\lambda}{\partial \lambda} \frac{\partial f}{\partial \lambda} \right] = 0$$

where q is the safety factor and terms of order ν have been neglected. From the definition of λ_c we see that the boundary layer occurs on a surface of constant

$$\lambda' \equiv \left[\frac{w}{(w - w_0)} \right) \lambda \,.$$

Thus the essential variation of f is given by

$$f(\lambda, w, \theta, \zeta) \approx f(\lambda', \theta, \zeta) \,,$$

whence

$$\left(\frac{R}{B} \right) \frac{\partial}{\partial \lambda} \left[\frac{u\lambda}{\partial \lambda} \frac{\partial f}{\partial \lambda} \right] \approx \left(\frac{R}{B} \right) u\lambda' \left[\frac{w}{(w - w_0)} \right] \frac{\partial^2 f}{\partial \lambda'^2} \approx \left(\frac{R}{B} \right) u_c \lambda'_c \left[\frac{w}{(w - w_0)} \right] \frac{\partial^2 f}{\partial \lambda'^2}$$

with

$$u_c = u(\lambda = \lambda_c) \approx [2w_0 + 2\varepsilon(w - w_0)(1 + \cos\theta)]^{1/2} \tag{8}$$

and

$$\lambda'_c \equiv \frac{1}{B_{\max}} \approx \left(\frac{1}{B_0} \right)(1 - \varepsilon) \,. \tag{9}$$

Here $\varepsilon = r/R_0$ denotes the inverse aspect ratio.

Note that the layer at $\lambda' = \lambda'_c$ occurs only for $w > w_0$. For simplicity we assume $\varepsilon w < w_0$, or

$$\frac{e\Phi}{T} > \varepsilon \, , \tag{10}$$

in order to expand

$$u_c \approx [2w_0]^{1/2} \left[1 + \varepsilon \left(\frac{(w - w_0)}{2w_0} \right) \, (1 + \cos\theta) \right] \, .$$

Then the collision term can be simplified, neglecting terms smaller than $\mathcal{O}(\varepsilon)$, with the result

$$\left(\frac{R}{B} \right) \, \frac{\partial}{\partial\lambda} \left[\frac{u\lambda}{\partial\lambda} \frac{\partial f}{\partial\lambda} \right] \approx [2w_0]^{1/2} \, R_0 \, B_0^{-2} \left\{ 1 + \varepsilon \left(\frac{w - 3w_0}{2w_0} \right) + a(w)\varepsilon\cos\theta \right\} \cdot \left[\frac{w}{(w - w_0)} \right] \frac{\partial^2 f}{\partial\lambda'^2}$$

where

$$a(w) = \frac{(w + 3w_0)}{2w_0} \, .$$

Here the second, θ-independent term in curly brackets gives only a small correction to the θ-averaged f; we will see that such corrections do not affect the particle flux. Thus, without significant loss of accuracy, the boundary-layer equation can be expressed as

$$\frac{\partial f}{\partial\zeta} + \left(\frac{1}{q} \right) \, \frac{\partial f}{\partial\theta} = \sigma(1 + \varepsilon a \cos\theta) \frac{\partial^2 f}{\partial x^2} \, , \tag{11}$$

where x is the boundary layer variable,

$$x = \left\{ B_0^2 \, \frac{(w - w_0)}{[\nu \, R_0 (2w_0)^{1/2}]} \right\}^{1/2} (\lambda' - \lambda'_c) \, . \tag{12}$$

Equation (11) is to be solved subject to the asymptotic boundary conditions given by (6) and (7). In terms of the variable x, these are "half-space conditions," in the sense of having distinct forms for $x > 0$ and $x < 0$. Problems involving half-space boundary conditions, although usually amenable to the Wiener-Hopf technique, are rarely straightforward. The present case is further complicated by explicit, and essential, θ-dependence — a dependence that turns out to be crucial to the pinch effect under investigation. Fortunately Eq. (11) has the same form as that derived previously for the case of magnetic asymmetry.[10] Thus the

8

previous solution can be adapted to the present case, taking into account differences in the coefficient of cos and in the structure of the boundary layer. We thus find that (11), (6) and (7) together imply

$$H = \left(\frac{\varepsilon a}{2} \right) \left[h(r, \theta, \zeta, w; q) \, e^{i\theta/q} + h(r, \theta, \zeta, w; -q) \, e^{-i\theta/q} \right] \tag{13}$$

where the x-independent function h is given by

$$h = -\alpha(w) e^{i/2q} |q| \sin\left(\frac{1}{q} \right) N(q) \left(\frac{eER}{T} \right) f_M \,, \text{for} \quad w > w_0 \,,$$

$$h = 0 \quad , \qquad w < w_0 \,. \tag{14}$$

with

$$\alpha(w) = \left\{ \frac{B_0^2 (w - w_0)}{[\nu R_0 (2 w_0)^{1/2}]} \right\}^{1/2} \,.$$

The function $N(q)$ is quite complicated, but slowly varying and of order unity.[10]

IV. Particle Flux

Here we use Eqs. (13) and (14) to compute the radial particle flux. The calculation is straightforward in principle, involving nothing more than substitution into the definition

$$\Gamma = \left\langle \int d^3 v \, f \, V_{dr} \right\rangle \,, \tag{15}$$

where the drift velocity is given by Eq. (2). However the sources of θ-dependence in the integrand are sufficiently numerous to justify a relatively detailed account. In particular we shall note some minor errors in Ref. 10.

To begin we express the flux surface average as

$$\langle A \rangle \equiv \frac{\oint d\theta \oint d\zeta \, \sqrt{g} \, A}{\left[\oint d\theta \oint d\zeta \, \sqrt{g} \right]}$$

9

where $\sqrt{g}$ is the spatial Jacobian,

$$\sqrt{g} = \frac{q \chi'(r) R^2}{I} \ .$$

Here $\chi' \approx R_0 \, B_{p0} \approx r B_0/q$ is the radial derivative of the poloidal flux, while $I(r)$ measures the symmetric toroidal field according to $B_T = I(r)/R$. The key feature of the average is its annihilation property:

$$\langle \mathbf{B} \cdot \nabla F \rangle = 0 \ ,$$

any single-valued function F. For the drift we use the identity

$$\mathbf{B} \times \nabla r = \frac{1}{\chi'} \left(I \mathbf{B} - R^2 \, B^2 \nabla \zeta \right) \ .$$

and Eq. (2) to conclude

$$\chi' V_{dr} = \left(\frac{Iu}{\Omega} \right) \mathbf{B} \cdot \nabla \left(\frac{u}{B} \right) - \frac{B^2 u}{\Omega} \left(\frac{\partial}{\partial \zeta} \right) \left(\frac{u}{B} \right) \ .$$

Then, since

$$\int d^3 v = 2\pi \sum_\sigma \int dw \, d\lambda \, \frac{w}{u} \ ,$$

we have

$$\chi' \Gamma = \left\langle 2\pi \sum_\sigma \int dw \, d\lambda \, w \left(\frac{B}{u} \right) f \left[\left(\frac{Iu}{\Omega} \right) \mathbf{B} \cdot \nabla \left(\frac{u}{B} \right) - \frac{B^2}{\Omega} \left(\frac{\partial}{\partial \zeta} \right) \left(\frac{u}{B} \right) \right] \right\rangle \ .$$

We evaluate both terms in this expression by partial integration. It is then seen that the first term can only contribute $\mathcal{O}(\nu)$ to Γ, since

$$\mathbf{B} \cdot \nabla f = \mathcal{O}(\nu) \ . \tag{16}$$

Thus, keeping to zeroth order in ν, we have

$$\chi' \Gamma = \left\langle 2\pi \sum_\sigma \int dw \, d\lambda \, w \left(\frac{B}{u} \right) \frac{\partial f^0}{\partial \zeta} \left(\frac{B^2 u}{\Omega} \right) \left(\frac{u}{B} \right) \right\rangle \ . \tag{17}$$

Here we used large aspect ratio to write $B \approx B_T = B_0(1 - \varepsilon \cos \theta)$, an approximation that makes $B^2 \sqrt{g}$ a flux function. Equations (6) and (7) show that only the trapped region

10

contributes to Γ, and (16) shows that we can replace $\partial f/\partial \zeta$ by $(-1/q)(\partial f/\partial \theta)$; thus (17) becomes

$$\Gamma = -\left(\frac{1}{B_0 r}\right)\left\langle 2\pi \sum_\sigma \int_t dw\, d\lambda\, w\, \frac{\partial f^0}{\partial \theta}\left(\frac{B^2 u_c}{\Omega}\right)\right\rangle \tag{18}$$

where the t-subscript reminds us to integrate only over the trapped region (in which $u \approx u_c$), and where we have recalled $\chi' = rB_0/q$.

Next we recall that $f^0 = H$ is independent of λ in the trapped region. It follows that the λ-integration gives simply

$$\int_t d\lambda = \left(\frac{1}{B} - \lambda_c\right) = \left(\frac{w_0}{wB_0}\right)\left[1 + \varepsilon\left(\frac{w}{w_0}\right)\cos\theta\right] . \tag{19}$$

Here, as in (11), we have neglected $\mathcal{O}(\varepsilon)$-corrections when they appear without θ-dependence; only the θ-dependent terms can affect the flux. A factor analogous to (19) was apparently omitted in Ref. 10.

We substitute (19) into (18), take into account the θ-variation of B as well as that implicit in the surface average, and find that

$$\Gamma = -\sqrt{2}\, w_0^{3/2}\left(\frac{mc}{2\pi e\, B_0 r}\right)\oint d\theta \oint d\zeta \sum_\sigma \int dw\, \frac{\partial H}{\partial \theta}\left\{1 + \varepsilon\left[\frac{(3w + w_0)}{2w_0}\right]\cos\theta\right\}$$

$$= -\left(\frac{3}{2}\sqrt{2}\,\pi\right)\left(\frac{mc}{eB_0 R}\right)\oint d\theta \oint d\zeta \sum_\sigma \int dw\, w_0^{1/2}\left(\frac{w + w_0}{3}\right)\frac{\partial H}{\partial \theta}\cos\theta . \tag{20}$$

The numerical coefficient in (20) corrects the corresponding expression in Ref. 10 [Eq. (74)], with regard to both the factor of (19) and an additional omission, in Ref. 10, of $\sqrt{2}$.

Finally we substitute from Eqs. (13) and (14) for H. The θ-integral is elementary and yields the q-dependent factor

$$K(q) = 3.3|N(q)|\left(\frac{q}{2\pi}\right)^2 \sin\left(\frac{2\pi}{q}\right)\sin\left(\frac{\pi}{q}\right) ,$$

which is graphed in Ref. 10. Its key features are clear: K changes sign at $q = 2$, being positive for $q > 2$. It is of order unity for $q \approx 2$.

The energy integral in Eq. (20), which differs markedly from the version in Ref. 10, yields a w_0-dependent factor

$$L(w_0) \equiv \left(\frac{1}{2}\right) \int_{x>x_0} dx e^{-x} \left(\frac{x}{x_0}\right)^{3/4} (x - x_0)^{1/2} \left(\frac{x + x_0}{3}\right) (x + 3x_0) , \qquad (21)$$

where $x_0 = mw_0/T = e\Phi_0/T$. L is most conveniently evaluated numerically, with the result sketched in Fig. 1. Note that L is quite large, $L \approx 10$, for $e\Phi_0/T$ of order unity. Indeed, L is easily seen to diverge as $x_0^{-3/4}$ for $x_0 \to 0$, although Eq. (10) makes this limit unphysical. On the other hand it decays exponentially for large Φ_0. The point here is that the boundary layer at $\lambda = \lambda_c$ exists only for particles with $w > w_0$; particles with $w < w_0$, electrostatically trapped for all λ, do not see a boundary layer and do not contribute to the enhanced pinch. Thus, because of the Maxwellian nature of f_0, the number of contributing particles becomes small for large Φ_0.

Hence the particle flux is expressed as

$$\Gamma = -4.47 \, K(q) \, L(\Phi_0) \left(\frac{r}{R}\right) \left(\frac{v_{th} \, \tau_e}{R}\right)^{1/2} cn \frac{E}{B} \qquad (22)$$

where $\tau_e = 1/\nu_e$ is the electron-ion collision time of Braginskii, and $v_{th} \equiv (2T_e/m_e)^{1/2}$ is the electron thermal speed. Because of the nature of the function K, this flux is inward for $q > 2$; it is outward but relatively small for $q < 2$, vanishing again at $q = 1$.

V.   Conclusions and Discussion

We have found that the induced toroidal electric field in a tokamak can interact with asymmetric electrostatic perturbations to drive rapid inward motion of the trapped particles. The resulting flux, given by Eq. (22), depends sensitively on the perturbation amplitude and on the safety factor, but can be stronger than the conventional (axisymmetric) Ware pinch, $\Gamma_w = -1.46 \, \varepsilon^{-1/2} \, q \, cnE/B$. Indeed, Eq. (22) can be expressed as

$$\Gamma \approx 3 \, K(q) \, L(w_0) \left(\frac{\varepsilon^{3/2}}{q\nu_{*e}}\right)^{1/2} \Gamma_w .$$

Here the factor $(\varepsilon^{3/2}/q\nu_{*e})^{1/2}$ will not be far from unity, even well into the banana regime; similarly $3K$ can be presumed close to one. However, as we have observed, the factor L is large at moderate amplitude, $e\Phi_0/T\tilde{<}1$. Hence, for small ν_* and $q \approx 3$, an inward pinch of several times the neoclassical[5] value can be reasonably estimated.

The physical origin of the asymmetric pinch is very different from that of the conventional trapped particle pinch effect.[5] It will be recalled that the latter, while modified by collisions, has it roots in the axisymmetic kinematics of trapped, collisionless particles. Equation (22) on the other hand, is a fundamentally collisional effect, reflecting collisional entrainment of trapped particles by untrapped ones. While trapped particles cannot contribute to Ohmic current, they are driven radially by collisional friction with the transiting, Ohmically accelerated particles. That the two types of pinch — symmetric and asymmetric — reflect quite different physics is clear from the fact that only the former is necessarily inwards. The direction of the asymmetric flux depends upon the safety factor, changing sign at $q = 2$.

Trapping in the potential bump will also drive outward fluxes, proportional to the density and temperature gradients. These contributions, however, will be diffusive in nature, and therefore in competition with neoclassical and turbulent diffusion. We have concentrated on the non-diffusive, inward flux because of its apparent role in the experimental observations, as discussed in Sec. I.

As a partial explanation of the observed pinching in tokamak experiments, our result has manifest defects. In particular, not all the observations are made in the low-collisionality regime we have assumed. Most importantly, our model for the spatial structure of the perturbation is obviously idealized; a realistic model would have numerous bumps, with appropriate θ-dependence. Particle-trapping effects in such a geometry would probably require numerical treatment.

Nonetheless, we believe the model captures crucial features of physical, small mode-number perturbations. Thus the observed frequencies of such fluctuations are typically well

less than the bounce frequency, and at least marginally less than the collision frequency, so our use of a steady state model is reasonable. With regard to the geometrical simplifications, it would appear that the crucial features of trapping and boundary layer formation would be preserved, as noted in Sec. I, by any perturbation whose parallel wave number does not vanish.

Finally we note that electrostatic symmetry breaking might result from external manipulation, rather than plasma instability. For example, toroidally localized fueling schemes (such as gas puffing) can lead to a transient electrostatic "bump," similar to that in our model. Since the introduced gas is relatively cold, it would not disperse along field lines until many transit and collision times of the ambient plasma had passed. Our model would roughly describe the intervening time period, and predict that trapped, banana-regime particles in the radial vicinity of the bump would drift inwards.

Acknowledgments

References

1. B. Coppi and N. Sharky, Nucl. Fusion **21**, 1363 (1981).

2. J.D. Strachan, N. Bretz, E. Mazzucato, C.W. Barnes, D. Boyd, S.A. Cohen, J. Hovey, R. Kaita, S.S. Medley, G. Schmidt, G. Tait, and D. Voss, Nucl. Fusion **22**, 1145 (1982).

3. S.K. Kim, D.L Brower, W.A. Peebles, and N.C. Luhmann, Jr., Phys. Rev. Lett. **60**, 577 (1988).

4. K.W. Gentle, B. Richards, and F. Waelbroeck, Plasma Phys. Controlled Fusion **29**, 1077 (1987).

5. A.A. Ware, Phys. Rev. Lett. **25**, 916 (1970).

6. L.R. Baylor, W.A. Houlberg, S.L. Milora, G.L. Schmidt, and Members of the JET-US DOE Pellet Collaboration, in IAEA *Tech. Committee Meeting on Pellet Injection and Toroidal Confinement*, (Gut Ising, 1988) (IAEA, Vienna, in press).

7. B. Coppi and C. Spight, Phys. Rev. Lett. **41**, 551 (1978).

8. W. Horton Phys. Fluids **19**, 711 (1976).

9. P.W. Terry, Phys. Fluids **B1**, 1932 (1989).

10. R.D. Hazeltine and M.N. Rosenbluth, Phys. Fluids **15**, 2211 (1972).

11. F.L. Hinton and R.D. Hazeltine, Rev. Mod. Phys. **48**, 239 (1976).

Figure Caption

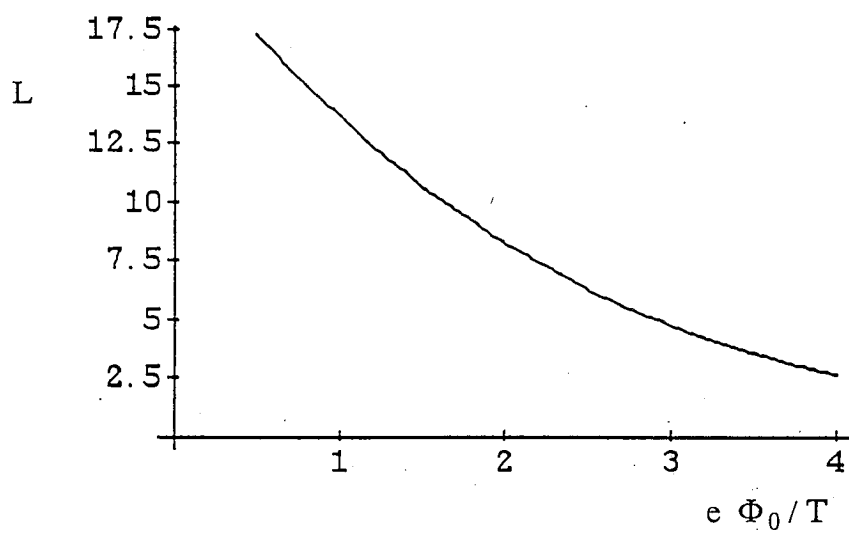The function L of Eq. (24). The abscissa measures the bump amplitude, $e\Phi_0/T$.

Figure 1